Experimental and Analytical Investigations of Jets Exhausting into a Deflecting Stream

J. C. Wu,* H. M. McMahon,† D. K. Mosher‡, and M. A. Wright‡
Georgia Institute of Technology, Atlanta, Ga.

A circular jet issuing normally from an infinite flat plate into a deflecting stream is treated by the use of a potential flow model which represents the flowfield surrounding the jet, exclusive of the wake. The results indicate that the entrainment of deflecting-stream fluid into the jet is important in determining the plate pressure and that, for the case where the jet speed is much higher than the deflecting-stream speed, it is possible to use a two-dimensional representation. The calculated plate pressure distribution is compared with results of experiments. Experimental results are presented for noncircular as well as circular jets exhausting at various jet velocities from a large flat plate. Results indicate that a streamwise jet exit configuration is desirable.

Nomenclature

a = radius of the circular jet orifice
C_p = plate pressure coefficient
C_s = interference force coefficient
K = dimensionless entrainment coefficient
m = sink strength
p_∞ = freestream static pressure
r = radial coordinate in plane of plate (Fig. 2)
R = upper limit of integration (Eq. 3)
V_j = jet exit velocity
V_∞ = freestream velocity
x = coordinate in freestream direction
x_s = sink location
z = coordinate normal to plate
β = angular coordinate in plane of plate (Fig. 2)
β_0 = upper limit of integration (Eq. 3)
θ = momentum thickness of plate boundary layer
ν = kinematic viscosity
ρ_j = jet exit density
ρ_∞ = freestream density

I. Introduction

During the last few years there has been an increasing emphasis on VTOL and STOL technology because of military and commercial needs. Jet-lift aircraft and aircraft using lift fans represent a means of achieving V/STOL capability. One important problem inherent in the design of such vehicles is the aerodynamic interference effect present during the transition phase of the flight, when the vehicle has attained some forward speed but still must rely on the jet or fan for much of its lift. During this critical phase the jet efflux interacts with the air flowing over the surface and the resulting interference can cause stability problems as well as a severe loss of lift.

This paper considers the interaction of a turbulent jet with a low-speed deflecting stream. The jet exhausts perpendicularly from the surface of a large flat plate into the deflecting stream. The case of the jet operating very near the ground is not considered here; that is, the jet is free to bend without impingement. Experimental results are presented for the plate pressure distribution and jet path for three different jet exit configurations. The jet velocity was varied in the experiment. Photographs of oil film traces on the plate surface are presented. The usefulness of a two-dimensional potential flow model representing the flow around a circular jet is considered, and pressure distributions calculated with this flow model are compared with experimental results. Several important factors involved in the interference between the jet and the deflecting stream are discussed.

Much detailed experimental work has been reported concerning the interaction of a circular jet with a subsonic deflecting stream, where the jet issues either from an exit set flush with a surface or from the end of a pipe immersed in the stream.[1–11] Considerable information exists on the gross effects of single and multiple jets of various exit geometries in wing-fuselage combinations.[12–18] Data on other than circular jets are generally restricted to results for jet penetration,[19,20] and to the authors' knowledge the only surface pressure data pertinent to the V/STOL problem is that reported in Ref. 21 for a rectangular jet orifice set in a wing surface. One of the objectives of the present research is to provide detail data for noncircular jets in order that the contrast between the circular and noncircular cases may give further insight into the interaction problem. In particular, the three configurations chosen represent different ratios of jet perimeter to jet width in the direction normal to the deflecting stream so that the effects of blockage and entrainment are varied.

The jet interference problem is so complex that it has thus far defied a detailed theoretical treatment. However, several analytical models[10,22,23] have been proposed which offer the possibility of predicting the interference effects based on some empirical information. The models have the common feature of using a potential flow representation of the interference flowfield, but differ in the manner in which the flowfield is represented and in the factors influencing the flowfield that are taken into account. In the present work, a relatively simple blockage-sink model is considered. The analysis presented differs from that of Ref. 10 in that an attempt is made to account for the effect of the blockage due to the presence of the wake and also, based on experimental observations, the entrainment of the deflecting-stream air into the jet is considered to take place mainly through the

Presented as Paper 69-223 at the AIAA/AHS VTOL Research, Design, and Operations Meeting, Atlanta, Ga., February 17–19, 1969; submitted March 11, 1969; revision received August 4, 1969. This work is supported by the U.S. Army Research Office, Durham, N. C., under contract DAHCO4 68 C0004. The authors gratefully acknowledge many stimulating and fruitful discussions with J. E. Hubbartt and the assistance of D. C. Seymour and J. G. Palfery in the experiments.

* Professor of Aerospace Engineering. Associate Fellow AIAA.
† Associate Professor of Aerospace Engineering. Member AIAA.
‡ Research Assistant, School of Aerospace Engineering.

wake rather than along the jet periphery. Numerical results obtained here are limited to the case where the jet velocity is sufficiently high in comparison with the deflecting stream velocity so that a two-dimensional approximation appears reasonable, i.e., insofar as the calculation of plate pressure distribution is concerned, the variation of flow between planes parallel to the plate is ignored.

II. Experiment

Apparatus and Procedure

The experiments were conducted in the Georgia Institute of Technology low-speed wind tunnel, which has a circular test section 9 ft in diam. A $\frac{3}{8}$-in. thick aluminum plate 48 in. × 66 in. was mounted 12 in. above the bottom of the test section (Fig. 1). A 32-in.-diam hole in the center of the plate (Fig. 2a) accepts a disk containing twelve 0.040-in.-diam pressure taps along a radius. This disk can be rotated remotely so that pressures can be measured along any ray. A 7-in.-diam hole in the center of this disk accepts a nozzle block which fits flush with the disk and the plate surface. Two jet nozzle blocks were made in order to change the jet exit geometry. Surface pressures very near the jet exit are measured by pressure taps in the nozzle block.

Air for the jet is supplied by a 100-hp centrifugal compressor. The air is led from the compressor through a 6-in.-diam line containing an orifice plate and a butterfly valve for setting jet exit conditions, through a 4-ft long straight section of 6-in. pipe, through three screens, and thence into the nozzle supply pipe.

The three jet exit configurations used in the experiments are shown in Fig. 2b. Configuration A is a circular jet for which data were available from previous investigations for comparison with present results. Configurations B and C use the same nozzle block and are an approximation of an elliptical jet exit. Configuration B has the major axis aligned parallel to the freestream and will be referred to as the streamwise configuration. Configuration C has the major axis aligned perpendicular to the freestream direction and will be referred to as the blunt configuration. All three configurations have the same exit cross-sectional area but represent different blockages to the freestream and present different interfaces with the freestream.

Surveys of total pressure, static pressure, and flow direction were made along several vertical lines in the plane of symmetry behind the jets. These quantities were obtained using a probe containing five pressure taps. The pitch angle of the flow is found directly by nulling the pressure difference

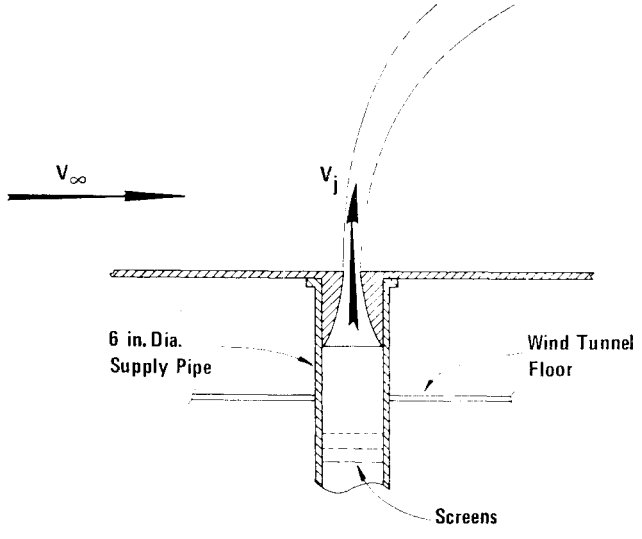

Fig. 1 Plate in a wind tunnel.

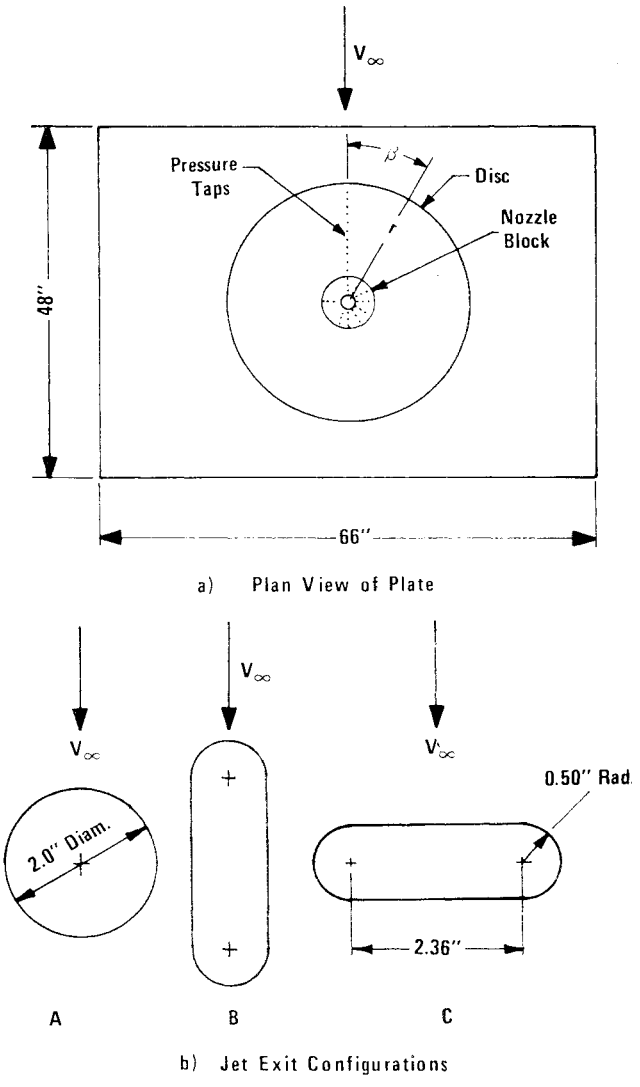

Fig. 2 Plate and jet configurations.

between two tap locations on the probe. The yaw angle is found by reference to a calibration curve.

As will be discussed later, for incompressible flow the interference phenomenon is primarily a function of the ratio of jet-to-freestream velocity. However, when compressibility of the jet flow becomes significant, an equivalent velocity ratio must be used which is the square root of the momentum flux ratio $(\rho_j V_j^2)^{1/2}/(\rho_\infty V_\infty^2)^{1/2}$. This parameter was varied through values of 4, 8, and 12 in the experiments. Under the present experimental conditions, the difference between this momentum flux parameter and the actual velocity ratio is small (6% or less). Thus, for simplicity, this parameter will be simply treated as the velocity ratio V_j/V_∞, in this paper. The results presented are for a freestream velocity of 50 fps.

Oil film flow visualization was done by covering the plate with white contact paper and applying a mixture of lamp black, oleic acid, and diesel fuel oil. The tunnel and jet flows were started and the plate observed until the pattern became established, at which time the flows were stopped and the oil pattern photographed.

All pressures were measured with a variable capacitance electric manometer calibrated against an alcohol micromanometer. The plate pressure measurements were accurate to within ±1% of the freestream dynamic pressure, and were repeatable within ±1%.

The tunnel wall boundary layer was measured and the plate was mounted sufficiently above the tunnel floor so that it was well outside the boundary layer. Checks were made to determine the disturbance of the flow above the

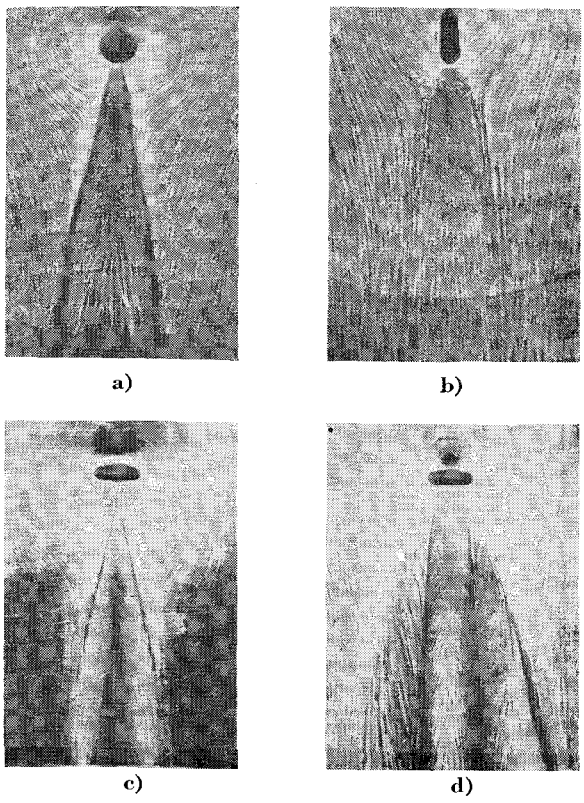

Fig. 3 Flow patterns on the plate: a) $V_j/V_\infty = 4$, b)$V_j/V_\infty = 4$, c) $V_j/V_\infty = 4$, d) $V_j/V_\infty = 12$.

plate due to the blockage of the flow underneath the plate. The disturbance was made negligible by adding fairings to the supporting structure underneath the plate. The boundary-layer velocity profile on the plate was measured on the centerline 15 in. from the leading edge and was found to follow the $\frac{1}{7}$ power law.

The jet exit velocity was set by controlling the total pressure in the supply pipe just before the jet nozzle contraction. The jet efflux as determined from the static-to-total pressure ratio, assuming the static pressure at the jet exit to be p_∞ and the nozzle discharge coefficient to be 100%, agreed within 1% with the values obtained from the orifice meter measurements and from the total pressure surveys in the jet exit plane.

The uniformity of the jet exit conditions for the three configurations was checked by making total and static pressure surveys in the jet plane with the tunnel off. Results

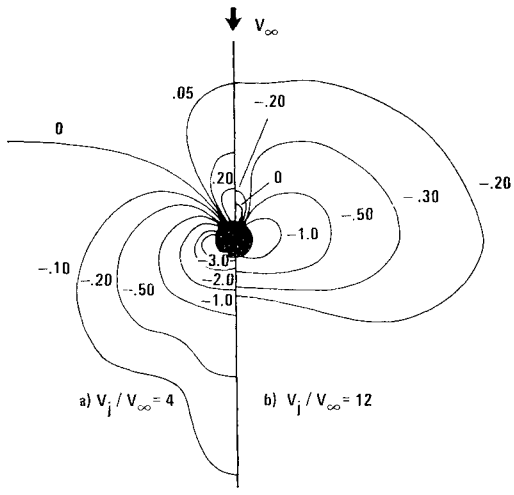

Fig. 4 Plate pressure coefficients around a circular jet.

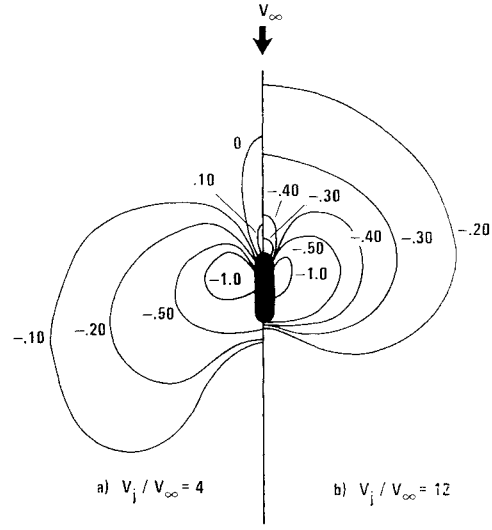

Fig. 5 Plate pressure coefficients around a streamwise jet.

showed a flat velocity distribution (less than 2% variation) over the jet cross section.

Discussion of Results

1. *Oil film tests*

The photographs of the oil film traces on the plate surface are shown in Fig. 3. The freestream velocity in all cases is directed from the top to the bottom of the photograph. The black diamond-shaped area directly up stream of the jet indicates a region where the flow near the plate surface decelerates due to the blockage by the jet and then accelerates around the sides of the jet. The light areas to the sides of the circular jet indicate relatively high-speed regions. Some streamlines bend toward the jet and terminate at the jet periphery, indicating entrainment of deflecting-stream air into the jet. The photographs also show a distinct wake region with some streamlines terminating at the edge of the wake, showing entrainment into the wake region. There is an area in the wake adjacent to the jet where the flow is toward the jet, as evidenced by the direction of motion of the oil film during the run. In some cases, two "lobes" can be observed in this area. The wake becomes broader as the velocity ratio is increased. It should be emphasized that oil film photographs are indicative of flow features near the plate and do not necessarily represent the flow pattern far from the plate.

2. *Static pressure distribution*

The static pressure distribution on the plate surface for various jet conditions is shown in Figs. 4, 5, and 6 and is presented in coefficient form. The static pressure coefficients were obtained by measuring the difference in static pressure at a point on the plate with and without jet flow and dividing the difference by the freestream dynamic pressure. The static pressure coefficient with the jet off was very uniform over the entire plate, the measured values deviating from the average value of 0.01 by less than 0.003.

The pressure distributions for the case of the circular jet are in excellent agreement with those reported in Ref. 6. The symmetry of the pressure distribution about the plate centerline with the jet on was found to be excellent from pressure measurements across the span of the plate.

It is seen that, for all three jet configurations, increasing the velocity ratio results in a lateral and forward spreading of

Table 1 Comparison of interference force

Configuration	Velocity ratio 4	8	12
Streamwise	0.93	1.39	1.70
Circular	1.00	2.07	2.24
Blunt	1.18	3.15	3.94

the low-pressure region. This is indicative of the increasing effect of entrainment. With increasing V_j/V_∞, the small region of positive pressure directly in front of the jet reduces in size and a suction region appears for the circular and streamwise jets at $V_j/V_\infty = 8$ and 12.

Comparing Figs. 4, 5, and 6 illustrates the effects of varying the jet exit configuration while keeping the velocity ratio constant (at 4 and 12). The trend here is a forward shift of the low-pressure region as the length-to-width ratio of the jet exit is increased. Also, the high-pressure region in front of the jet is considerably reduced in size as the jet becomes less blunt. These effects are more pronounced for the higher velocity ratio cases. The wake behind the jet has a very important influence on the plate pressure distribution. The importance of this influence increases with the bluntness of the jet exit geometry.

The pressure coefficients were integrated over the area between the jet and $r = 16$ in. The resulting suction force in each case was divided by the value for the circular jet at a velocity ratio of 4. The results are shown in Table 1.

For each configuration, the plate suction force coefficient increases with increasing V_j/V_∞. This dependence becomes weak at the larger values of V_j/V_∞. It should be noted, however, that the plate suction force becomes a smaller percentage of the jet momentum as V_∞ decreases while V_j is held constant. At a given constant value of V_j/V_∞, the plate suction force coefficient decreases with decreasing jet bluntness. For the higher velocity ratio cases, the decrease is very pronounced, while for the case $V_j/V_\infty = 4$, there is only a slight decrease.

3. *Jet plume measurements*

The jet centerline paths for the three jet configurations at a velocity ratio of 8 are presented in Fig. 7. The paths shown represent the lines of maximum total pressure in the plume as determined by surveys with the pressure probe. The path for the circular jet agrees well with that given by Ref. 2.

It is seen that penetration increases with increasing length-to-width ratio of the jet. This was observed for all three velocity ratios (4, 8, and 12) tested. The streamwise jet initially has a greater interface between the jet and the deflecting stream than does the circular jet and thus is expected to have a greater entrainment of freestream air. From the point of view of the entrained momentum, the streamwise jet should deflect more than the circular jet. The fact that the reverse is true suggests that the observed trend is primarily due to a decreasing aerodynamic drag with a decreasing jet bluntness. It was also observed that penetration increases with increasing velocity ratio for each of the three configurations.

The velocity field in the plane of symmetry in and behind each of the three jet plumes was measured with the pressure probe at a velocity ratio of 8, and the results presented in the preprint version of this paper. These measurements indicate an extensive region of low total pressure behind the jet plume. However, neither the origin of the wake nor the character of the flow in the wake has been established. Flow visualization indicates that the wake is unsteady and very erratic. Further detailed studies of the wake region are necessary.

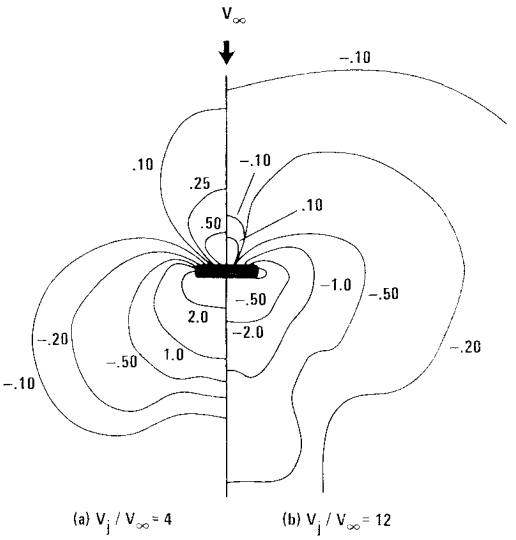

Fig. 6 Plate pressure coefficients around a blunt jet.

III. Analysis

Preliminary Considerations

The case here analysed is that of an incompressible jet issuing from a circular orifice located in an infinite flat plate. This restricted problem contains the major features of the interference flow problem. It is expected that a successful analytical approach for the restricted problem will lead to extensions applicable to more general problems.

It has been observed in the present work and in Refs. 2 and 4 that the presence of the jet leads to a separation of the deflecting stream behind the jet. The combined effects of aerodynamic forces acting on the jet and the entrainment of the deflecting-stream fluid into the jet, which carries momentum with it, causes the jet to spread, deform, and deflect. In turn, the jet interferes with the flow of the deflecting stream by displacing it, entraining it, and causing the separa-

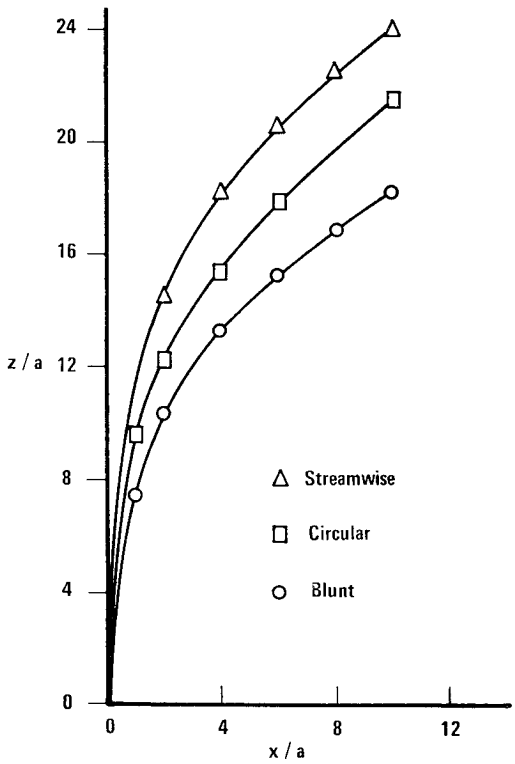

Fig. 7 Jet centerline paths for $V_j/V_\infty = 8$.

Table 2 Calculated force coefficient with entrainment

R	Wake included ($\beta_0 = \pi$)		Wake excluded ($\beta_0 = \frac{3}{4}\pi$)	
	Calculated ($K = 1$)	Experiment	Calculated ($K = 1$)	Experiment
5	−6.6	−17	−11.0	−14
10	−8.8	−38	−20.4	−33
15	−10.2	−55	−28.8	−48

tion region to form. These three factors are referred to as the blockage effect, the entrainment effect, and the wake effect, respectively.

Regarding the separation of the deflecting stream behind the jet, Bradbury and Wood[6] suggested that this is due to the plate boundary-layer air being drawn into the jet. Pressure measurements by Jordinson[2] and also in the present work show, however, that the low total pressure region behind the jet extends at least several jet diameters away from the plane of the plate. These observations suggest that the wake region is extensive and that the main stream also separates.

Dimensional analysis shows that, for the restricted problem under consideration the interference plate pressure coefficient C_p is dependent on only three dimensionless parameters, the ratio of the jet velocity to the undisturbed deflecting-stream velocity V_j/V_∞, the ratio of the momentum thickness to the jet orifice radius θ/a, and the jet efflux Reynolds number $V_j a/\nu$. In most applications of interest, the value of θ/a is of the order of 0.1, and variations in the momentum thickness of the plate boundary layer are expected to be of secondary importance[6] to the interference pressure. Furthermore, it may be argued that, if the jet efflux Reynolds number is sufficiently large, flow separation and other viscous effects in the interference flow may be insensitive to the variation of the Reynolds number. Plate pressure data from different sources, e.g., Refs. 5, 6, and the present work, obtained under diverse experimental conditions seem to support this argument. Although the Reynolds number range for which the above conclusion is valid has not been clearly established, it appears that in cases of practical interest the interference plate pressure is primarily a function of the velocity ratio V_j/V_∞ alone. This conclusion is further supported by the fact that experimental formulae[4,6,11] accurately describing the jet deflection path have been established as a function of the velocity ratio V_j/V_∞ alone.

It should be noted that the weak dependence of the interference pressure on the variation of the Reynolds number does not imply that the role of viscosity in the interference problem is negligible. Inasmuch as there exists a significant wake region, viscous effects are important. The insensitivity of the interference pressure to the variation of θ/a, however, tends to support the argument that the separation of the main deflecting stream is very important in the formation of the wake.

There has been little analytical effort dealing with the spreading and deformation of the jet in the deflecting stream. Recently, however, some attention has been given to the possibility of extending the early work of Lu,[24] which dealt with the time-dependent problem of the deformation of a circular column of fluid in a two-dimensional flow, to the three-dimensional steady flow problem of a jet in a deflecting stream. There are several semiempirical analyses concerned with the jet deflection path. Good agreement between semiempirical results and empirical jet paths was reported by Vizel and Mostinskii[25] considering only the aerodynamic drag on the jet, and by Keffer and Baines[4] considering only the entrained momentum. It appears that since the effects of aerodynamic drag and entrained momentum are both directly related to the deflecting-stream dynamic head, these two effects cannot be distinguished from one another by examining the jet path alone. In analytical studies of the interference plate pressure, it is necessary to know the importance of the entrainment factor. Presently available data are insufficient to permit a quantitative assessment of the importance of entrainment. Nevertheless, since some semi-empirical analyses[25] ignoring the entrained momentum require the postulation of excessively large drag coefficients, it appears that the entrained momentum does contribute significantly to the deflection of the jet.

Analytical Model

Although viscous effects are important in the wake formation and in determining the rate of entrainment into the jet, the flow of the deflecting stream outside the wake is essentially inviscid. Thus, it should be possible to construct a potential flow model to represent the deflecting-stream flow, exclusive of the wake region, by using doublets, vortices, and sinks to simulate the blockage and entrainment effects due to the presence of the jet. Because of the present uncertainty concerning the character of the wake, analytical study of the flow in the wake region must await further detailed experimental investigations.

The "blockage-sink" representation has the advantage of being simple and readily interpretable. Bradbury and Wood[6] argued that this simple representation is inadequate since, with the sink strength comparable in magnitude to that for a jet exhausting into stationary atmosphere, the model cannot produce an integrated suction force coefficient on the plate (lift loss) indicated by experiments. However, in the analysis of Bradbury and Wood,[6] as well as those of several other investigators,[10,17,22,23] the entire deflecting-stream flow was considered to be inviscid. As previously noted, experiments show the existence of an extensive region of low total pressure behind the jet. The constant total pressure potential flow representation of the entire deflecting stream therefore appears to be too strong a requirement. The question then arises as to what region of the flow is influenced by the wake, i.e., what portion of the flow should be excluded from a potential flow model? In the present analysis, a region downstream of the jet covering a total angle of 90° is excluded, and much better, in fact very promising, agreement with experimental data results. This excluded region is referred to as the wake region.

The necessity of excluding the wake region in the blockage-sink representation is demonstrated by considering a simple two-dimensional model with a line doublet and a line sink placed along the z axis, simulating, respectively, the blockage and the entrainment due to the presence of jet. The plate pressure coefficient for this flow is

$$C_p = -(a/r)^4 + 2K\cos\beta(a/r)^3 + (2\cos 2\beta - K^2)(a/r)^2 - 2K\cos\beta(a/r) \quad (1)$$

where K is the dimensionless entrainment coefficient defined by

$$K = m/2\pi a V_\infty \quad (2)$$

and m is the sink strength, representing the volume of air entrained into the jet per unit time per unit length of the jet.

Table 3 Calculated force coefficient omitting entrainment

R	Wake included ($\beta_0 = \pi$)		Wake excluded ($\beta_0 = \frac{3}{4}\pi$)	
	Calculated ($K = 0$)	Experiment	Calculated ($K = 0$)	Experiment
5	−1.5	−17	−2.7	−14
10	−1.6	−38	−3.5	−33
15	−1.6	−55	−3.9	−48

The integrated force coefficient for the area $1 \leq r/a \leq R$ and $0 \leq \beta \leq \beta_0$ is defined by

$$C_s = \int_0^{\beta_0} \int_1^R C_p \frac{r}{a} d\frac{r}{a} d\beta \tag{3}$$

For the case considered, the force coefficient is

$$C_s = \left(\frac{1}{2R^2} - \frac{1}{2} - K^2 \ln R\right) \beta_0 + 2K\left(2 - R - \frac{1}{R}\right) \times \sin \beta_0 + \ln R \sin 2\beta_0 \tag{4}$$

For the case of a freejet exhausting into a stationary atmosphere ($V_\infty = 0$) the appropriate dimensionless entrainment parameter is $m/(2\pi a V_j)$. Experimental data[26] for this freejet case gives $m/(2\pi a V_j) \cong 0.08$. For the case of a jet in a deflecting stream, $m/(2\pi a V_j) = KV_\infty/V_j$. With $V_j/V_\infty = 8$, the convenient value of $K = 1.0$ corresponds to $m/(2\pi aV_j) = 0.125$, which is comparable in magnitude to the freejet value.

Using $K = 1.0$, C_s values were calculated for $\theta = 3\pi/4$ (excluding the wake region) and π (including the wake region) for $R = 5$, 10, and 15. The calculated C_s values are compared with experimental values for the velocity ratio $V_j/V_\infty = 8$ in Table 2.

Table 2 shows that the calculated C_s values including the wake region are much smaller than the experimental values, while the values excluding the wake region are of the proper magnitude.

Values of C_s omitting the entrainment effect ($K = 0$) were also calculated. The results are presented in Table 3.

This table shows that the calculated values, even excluding the wake region, are much too small.

As shown previously, if the wake region is excluded, the contribution from entrainment is very important. Since there is little justification in the use of a potential flow model including the wake region, the neglect of the entrainment factor in some analytical models does not appear to be justified.

In order to study the usefulness of the blockage-sink representation in determining the flow details outside the wake region, a two-dimensional model was used to calculate the distribution of the interference pressure on the plate. It is recognized that the jet interference problem is basically three-dimensional and the results of a two-dimensional analysis can at most be approximate. Nevertheless, the simplicity resultant from the use of a two-dimensional model makes the approach attractive. To determine the range of V_j/V_∞ for which the two-dimensional representation may be reasonable, the effects of jet deformation, jet deflection, and variation of entrainment rate along the jet path, none of which can be accounted for in the two-dimensional model, were examined.

Existing experimental information[10] indicates that the change of jet shape (from a circle at the orifice to a characteristic kidney form) takes place in the region $0 \leq z/a \leq 0.6\ V_j/V_\infty$. Noting that the velocity induced at a given point in the flowfield by a three-dimensional blockage or sink element is inversely proportional to the square of the distance between the point and the element, it is expected that in regions close to the orifice the influences of the jet shape change and the entrainment rate change are not severe for velocity ratios $V_j/V_\infty \geq 8$. Far from the orifice, these three-dimensional effects may be more significant.

To detect the three-dimensional effects of jet deflection, the empirical jet centerline formula[23] $x/a = B(\cosh z/aB - 1)$, where $B = 0.38\ (V_j/V_\infty)^2$, was used. It is seen that for $V_j/V_\infty \geq 8$, the jet deflects less than one radius at a plane six radii away from the plate surface. It thus appears that the effect of jet deflection is not severe for $V_j/V_\infty \geq 8$. To verify this, the plate pressure distribution was computed using a large number of three-dimensional doublets and sinks

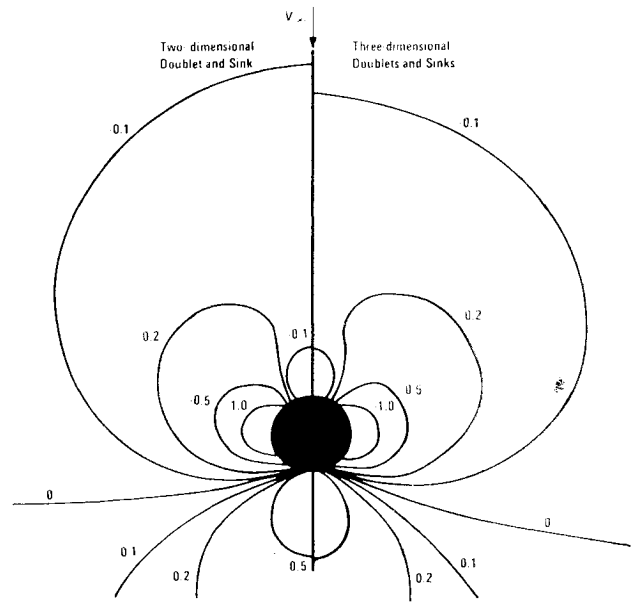

Fig. 8 Effect of jet path on pressure distribution.

distributed along the jet centerline path given by the above formula for the case $V_j/V_\infty = 8$. The resulting plate pressure distribution is compared in Fig. 8 with that obtained for the corresponding simple two-dimensional doublet-sink model. It is seen that the effect of jet deflection is indeed very small for the case $V_j/V_\infty = 8$. For $V/_jV_\infty > 8$, the jet deflects even less and the effects of jet deflection are expected to be less significant.

The simple doublet-sink model involves only one empirical parameter K. An attempt was made to establish a trend for the variation of the entrainment rate with the velocity ratio V_j/V_∞. Directly upstream of the jet, $\beta = 0$, the pressure coefficient is

$$C_p = -(a/r)^4 + 2K(a/r)^3 + (2 - K^2)(a/r)^2 - 2K(a/r) \tag{5}$$

C_p values calculated using this expression were matched with experimental values from several references to deduce the value of K. Unfortunately, the values obtained are drastically scattered so that it is difficult to draw any constructive conclusions regarding the trend. However, the general trend of the present data and that of Bradbury and Wood[6] indicate that entrainment increases with velocity for $4 \leq V_j/V_\infty \leq 12$ and is of the same order of magnitude as freejet entrainment.

Discussion of Results

Pressure distributions on the plate were calculated using the simple two-dimensional doublet-sink model, with the strength of the sink selected so that the pressure along the line $\beta = 0$ agreed with experimental values. The results agreed with the experimental data only in a region very close to the orifice. A more elaborate two-dimensional model was considered next in order to determine if the region of agreement could be extended.

To simulate the effect of blockage due to the wake, an afterbody was added to the circular cylinder. A Rankine oval of axis ratio 5.8 placed in a uniform stream in a complex ζ plane was transformed by the relation, $\zeta = \xi + 1/\xi$ to a circular cylinder with an afterbody placed in a uniform stream in the ξ plane. The complex potential in the ξ plane was obtained. Experimental observations indicate that a certain amount of deflecting-stream air is drawn into the wake region. This suggests that the entrainment effect is better represented as a distribution of sinks extending into the wake region. To simplify the analysis, a single sink

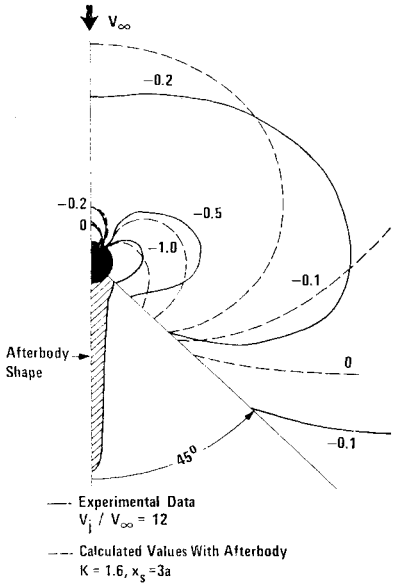

Fig. 9 Plate pressure distribution.

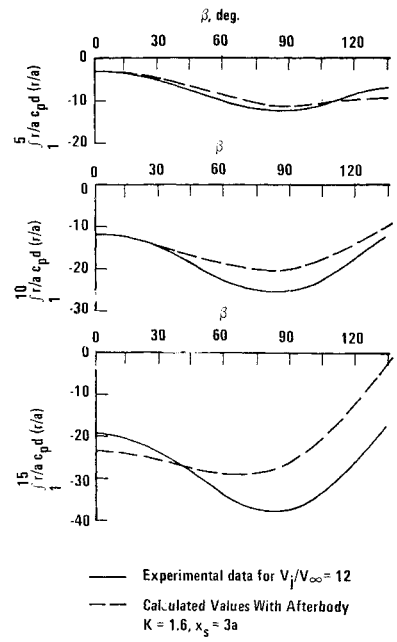

Fig. 10 Distribution of surface force around jet.

located at a distance x_s downstream of the origin was used to represent the combined effect of jet and wake entrainment. The strength and the location of the sink were adjusted to fit the pressure coefficient directly upstream of the jet, along the line $\beta = 0$. Pressure coefficient and surface force distributions for the combined cylinder-afterbody and sink configuration were calculated. The results with $K = 1.6$ and $x_s = 3a$ are compared with experimental values for $V_j/V_\infty = 12$ in Fig. 9. Some improvement over the results obtained with the simple doublet-sink model was noted. The surface force distribution around the jet, given by

$$\int_1^R \left(\frac{r}{a}\right) C_p d\left(\frac{r}{a}\right)$$

was evaluated as a function of β for $R = 5$, 10, and 15. The results are shown in Fig. 10. Very good agreement is observed in terms of the surface force distribution for the range $0 \leq \beta \leq 120°$.

In assessing the usefulness of the blockage-sink model, the following points are noted.

In the two-dimensional analysis, the effects of wake blockage and entrainment into the wake have been represented with some success by an afterbody containing a lumped sink effect for the jet and the wake. However, the calculation of the pressure distribution within the wake region has not been performed since it must await further experimental information. In view of the rather drastic simplification imposed on the two-dimensional model, the observed agreement between the calculated pressure distribution and the experimental data for the circular jet in a significantly large region near the jet exit is encouraging.

An extension of the two-dimensional blockage-sink model to three dimensions should present no computational difficulties, as has been illustrated by the computation leading to Fig. 8. For $V_j/V_\infty < 8$, because of the rapid deflection of the jet, three-dimensional effects are expected to be important. Such an extension will enable the inclusion of the effect of jet deflection and deformation as well as the variation of entrainment rate and wake geometry along the jet path. The extension, however, will require the specification of a number of additional empirical parameters which presently are of uncertain magnitude. In addition, experimental observations indicate that the jet plume deforms to a kidney shape containing a pair of vortices. The effects of the vortex-pair will be felt through additional entrainment into the jet and vortex-induced velocity around the jet. It is not clear at the present time to what extent these effects are important as regards the plate pressure. Thus, a three-dimensional extension of the blockage-sink model should be preceded by an investigation of this point.

Another extension of the two-dimensional blockage-sink model is the application of the model to other than circular jet exit configurations to study the relative importance of entrainment and blockage of the deflecting stream by the jet. This is presently in progress.

IV. Concluding Remarks

Experimental results for the plate pressure distribution for streamwise, circular, and blunt jet exit configurations and different values of V_j/V_∞ indicate that the relative importance of entrainment increases with increasing V_j/V_∞ and decreasing bluntness. The relative importance of the wake behind the jet increases with increasing jet bluntness. The suction force coefficient, with the data nondimensionalized by the freestream dynamic pressure, increases with increasing V_j/V_∞. The suction force coefficient decreases with decreasing jet bluntness, so that a streamwise jet exit configuration appears desirable.

A two-dimensional blockage-sink model yields a satisfactory plate pressure distribution in a significantly large region near the exit of a circular jet, provided that a region containing the wake is excluded. The analysis indicates that the entrainment factor is important in the interference problem.

References

[1] Callaghan, E. and Ruggeri, R., "Investigation of the Penetration of an Air Jet Directed Perpendicularly to an Air Stream," TN 1615, June 1948, NACA.

[2] Jordinson, R., "Flow in a Jet Directed Normal to the Wind," R & M 3074, Oct. 1956, British Aeronautical Research Council.

[3] Gordier, R., "Studies of Fluid Jets Discharging Normally into Moving Liquid," Technical Paper 28, Series B, 1959, St. Anthony Falls Hydro Lab., Univ. of Minnesota.

[4] Keffer, J. F. and Baines, W. D., "The Round Turbulent Jet in a Cross Wind," *Journal of Fluid Mechanics*, Vol. 15, Pt. 4, 1963, pp. 481–496.

[5] Vogler, R. D., "Surface Pressure Distribution Induced on a Flat Plate by a Cold Air Jet Issuing Perpendicularly from the Plate and Normal to a Low Speed Free Stream Flow," TN D-1629, March 1963, NASA.

[6] Bradbury, L. J. S. and Wood, M. N., "The Static Pressure Distribution Around a Circular Jet Exhausting Normally from a

Plane Wall into an Airstream," TN Aero 2978, Aug. 1964, British Royal Aircraft Establishment.

[7] Gelb, G. H. and Martin, W. A., "An Experimental Investigation of the Flow Field about a Subsonic Jet Exhausting into a Quiescent and a Low Velocity Air Stream," *Canadian Aeronautics and Space Journal*, Vol. 12, No. 8, Oct. 1966, pp. 333–342.

[8] Crowe, C. T. and Riesebieter, H., "An Analytic and Experimental Study of Jet Deflection in a Cross-Flow," *Fluid Dynamics of Rotor and Fan Supported Aircraft at Subsonic Speeds*, Advisory Group for Aerospace Research and Development Preprint, Paris, 1967.

[9] Pratte, B. D. and Baines, W. D., "Profiles of the Round Turbulent Jet in a Cross Flow," *Proceedings of the ASCE, Journal of the Hydraulics Division*, Vol. 92, No. HY6, Nov. 1967, pp. 53–64.

[10] Wooler, P. T., Burghart, G. H., and Gallagher, J. T., "The Pressure Distribution on a Rectangular Wing with a Jet Exhausting Normally into an Airstream," *Journal of Aircraft*, Vol. 4, No. 6, Nov.-Dec. 1967, pp. 537–543.

[11] Margason, R. J., "The Path of a Jet Directed at Large Angles to a Subsonic Free Stream," TN D-4919, Nov. 1968, NASA.

[12] Hickey, D. and Hall, L., "Aerodynamic Characteristics of a Large-Scale Model with Two High Disc-Loading Fans Mounted in the Wing," TN D-1650, Feb. 1963, NASA.

[13] Vogler, R. D., "Interference Effects of Single and Multiple Round or Slotted Jets on a VTOL Model In Transition," TN D-2380, Aug. 1964, NASA.

[14] Vogler, R. D., "Ground Effects on Single- and Multiple-Jet VTOL Models at Transition Speeds over Stationary and Moving Ground Planes," TN D-3213, Jan. 1966, NASA.

[15] Gentry, G. L. and Margason, R. J., "Jet-Induced Lift Losses on VTOL Configurations Hovering In and Out of Ground Effect," TN D-3166, Feb. 1966, NASA.

[16] Margason, R. J., "Jet-Induced Effects in Transition Flight," SP-116, April 1966, NASA.

[17] Williams, J. and Wood, M. N., "Aerodynamic Interference Effects with Jet-Lift V/STOL Aircraft under Static and Forward-Speed Conditions," *Zeitschrift für Flugwissenshaften*, Vol. 15, No. 7, July 1967, pp. 237–256.

[18] Margason, R. J. and Gentry, G. L., "Aerodynamic Characteristics of a Five-Jet VTOL Configuration in the Transition Speed Range," TN D-4812, Oct. 1968, NASA.

[19] Ruggeri, R., Callaghan, E., and Bowden, D., "Penetration of Air Jets Issuing from Circular, Square, and Elliptical Orifices Directed Perpendicularly to an Air Stream," TN 2019, Feb. 1950, NACA.

[20] Hardy, W. G., "Non-Parallel Flow Interactions," M.A.E. thesis, Univ. of Virginia, 1967.

[21] Peake, D. J., "The Pressures on a Surface Surrounding a Jet Issuing Normal to a Mainstream," Aero. Rept. LR-410, Nov. 1964, National Research Council of Canada, Ottawa, Canada.

[22] Monical, R. E., "A Method of Representing Fan-Wing Combinations for Three-Dimensional Potential Flow Solutions," *Journal of Aircraft*, Vol. 2, No. 6, Nov.-Dec. 1965, pp. 527–530.

[23] Wooler, P. T., "On the Flow Past a Circular Jet Exhausting at Right Angles from a Flat Plate or a Wing," *Journal of the Royal Aeronautical Society*, Vol. 71, March 1967, pp. 216–218.

[24] Lu, H. C., "On the Surface of Discontinuity Between Two Flows Perpendicular to Each Other," Engineering Rept. 4, Oct. 1948, National Tsing Hua University.

[25] Vizel, Y. M. and Mostinskii, I. L., "Deflection of a Jet Injected into a Stream," *Journal of Engineering Physics*, Vol. 8, No. 2, Feb. 1965, pp. 238–242.

[26] Ricou, F. P. and Spalding, D. B., "Measurements of Entrainment by Axi-Symmetrical Turbulent Jets," *Journal of Fluid Mechanics*, Vol. 11, Part I, Aug. 1961, pp. 21–32.

JAN.-FEB. 1970 J. AIRCRAFT VOL. 7, NO. 1

A V/STOL Wind-Tunnel Wall Interference Study

CHING-FANG LO* AND TRAVIS W. BINION JR.†
Arnold Air Force Station, Tenn.

An integrated theoretical and experimental study of slotted wall tunnels is described. Theoretical calculations based on a modification of the point-matching method with equivalent homogeneous boundary conditions have been used to show the relationship between the lift- and blockage-interference factors and wall porosity. Experimental interference factors are obtained by comparing lift coefficient vs angle of attack data obtained in a 30 × 45 in. tunnel with those from a 7 × 10 ft tunnel. Theoretical results indicate that the lift interference for conventional models is insensitive to the porosity of the vertical walls for a height to width ratio less than 0.8. It is shown that certain combinations of vertical and horizontal wall slots give simultaneous zero lift and blockage interference. The discrepancy between theoretical and experimental results may be caused by nonhomogeneous slots and viscous effects.

Nomenclature

a = width of slot
A_m, B_m = series coefficient constants
b = tunnel semiwidth
C = cross-sectional area of tunnel
C_L = lift coefficient
h = tunnel semiheight
I_m = modified Bessel function of the first kind of order m
K_0, K_1 = modified Bessel function of the second kind of order 0 and 1, respectively
k = geometric slot parameter, $l/\pi \ ln(\csc \pi a/2l)$
l = slot spacing
M_r = doublet strength
n = normal outward at the wall
P = nondimensional slot parameter, $(l + k/h)^{-1}$
R = viscosity parameter
S = wing area
s = wing span
U = freestream velocity
u = interference velocity in longitudinal direction

Presented as Paper 69-171 at the AIAA 7th Aerospace Sciences Meeting, New York, January 20–22, 1969; submitted February 20, 1969; revision received August 4, 1969. The research reported in this paper was sponsored by the Arnold Engineering Development Center, Air Force Systems Command, under Contract No. F40600-69-C-0001-SA10 with ARO Inc. Further reproduction is authorized to satisfy the needs of the U. S. Government.

* Research Engineer, Propulsion Wind Tunnel Facility. Member AIAA.

† Research Engineer, Propulsion Wind Tunnel Facility.